Subradiant-to-Subradiant Phase Transition in the Bad Cavity Laser

Athreya Shankar,[1,2,*] Jarrod T. Reilly,[3] Simon B. Jäger,[3] and Murray J. Holland[3]
[1]Center for Quantum Physics, Faculty of Mathematics, Computer Science and Physics, University of Innsbruck, Innsbruck A-6020, Austria
[2]Institute for Quantum Optics and Quantum Information, Austrian Academy of Sciences, Innsbruck A-6020, Austria
[3]JILA, NIST, and Department of Physics, University of Colorado Boulder, Boulder, Colorado 80309, USA

(Received 12 March 2021; accepted 8 July 2021; published 13 August 2021)

We show that the onset of steady-state superradiance in a bad cavity laser is preceded by a dissipative phase transition between two distinct phases of steady-state subradiance. The transition is marked by a nonanalytic behavior of the cavity output power and the mean atomic inversion, as well as a discontinuity in the variance of the collective atomic inversion. In particular, for repump rates below a critical value, the cavity output power is strongly suppressed and does not increase with the atom number, while it scales linearly with atom number above this value. Remarkably, we find that the atoms are in a macroscopically entangled steady state near the critical region with a vanishing fraction of unentangled atoms in the large atom number limit.

DOI: 10.1103/PhysRevLett.127.073603

Introduction.—Progress in laser physics has revolutionized our day-to-day lives and the scope of experiments across the entire spectrum of scientific disciplines. At its core, the laser is a highly out-of-equilibrium system whose steady state is maintained via a balance of driving and dissipation. A typical laser model involves a collection of continuously pumped two-level atoms interacting with an electromagnetic field confined in a cavity with lossy mirrors. In particular, bad cavity lasers operate in a regime where the lifetime of the photon is short compared to the effective lifetime of the upper atomic level [1–3]. Over the past decade, they have garnered significant attention because in these systems the sensitivity of the laser linewidth to cavity frequency fluctuations is strongly suppressed [1,4]. Furthermore, this narrow linewidth coexists in a regime where the emission amplitudes of the atoms can constructively interfere and give rise to superradiant emission. Apart from its promising technological potential, the superradiant regime has also been shown to host a variety of many-body phenomena such as synchronization [5–15], collective cooling [16–21], and self-organization [16,22–26].

In contrast, the regime preceding the onset of superradiance has received far less attention, partly because within the framework of mean-field theory the atoms appear to be in a trivial unpolarized product state. Prior beyond-mean-field studies have only considered this regime in passing [2,27] or for a small number of emitters [28,29], but have nevertheless demonstrated that the atoms populate collective dark states giving rise to steady-state subradiance. However, the physics in this regime and the stability of the highly correlated quantum states remain poorly understood especially given the fact that this regime is complementary to the well studied and much anticipated steady-state superradiant regime.

In this Letter, we show that the subradiant regime of a bad cavity laser is in itself a playground for a rich variety of physical phenomena. In particular, we show that the onset of superradiance is preceded by a dissipative phase transition between two distinct types of subradiance. The transition is shown to arise as a consequence of the bounded state space of the collective atomic system. The two subradiant steady states correspond to the population of different regions of this state space (see Fig. 1). The phase transition is heralded by a nonanalytic change in the cavity output power and a discontinuous change in a squeezing parameter. An experimentally attractive feature is the scaling of the output power, which is strongly suppressed and does not increase with atom number N below the critical point but instead scales linearly with N above this point. Near the critical point, we find that the atoms are in a macroscopically entangled state and that the fraction of unentangled atoms is vanishingly small as the number of atoms increases. From the viewpoint of dissipative spin models, this phase transition and the accompanying entanglement are striking because they arise in a model whose governing master equation contains no Hamiltonian terms but only Lindblad dissipators.

Model.—Our system consists of N atoms each with upper and lower levels $|\uparrow\rangle$ and $|\downarrow\rangle$, respectively, and a single lossy cavity mode as shown in Fig. 1(a). The atoms can be modeled using the language of Pauli matrices where $\hat{\sigma}_j^- = |\downarrow\rangle_j\langle\uparrow|_j (\hat{\sigma}_j^+ = |\uparrow\rangle_j\langle\downarrow|_j)$ is the lowering (raising) operator for atom j and $\hat{\sigma}_j^z = |\uparrow\rangle_j\langle\uparrow|_j - |\downarrow\rangle_j\langle\downarrow|_j$ is the population difference between the spin states. The finite lifetime of $|\uparrow\rangle$ causes atoms to emit photons both into free

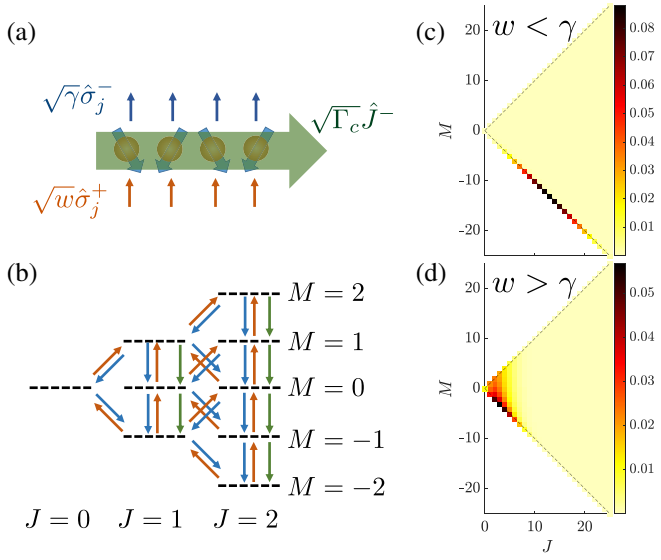

FIG. 1. (a),(b) Bad cavity laser model illustrated with $N=4$ atoms. The atoms undergo collective decay (green) in the presence of noncollective pumping (red) and additional noncollective decay (blue). When $w<\gamma+\Gamma_c$, the phases of the spins are anticorrelated, leading to steady-state subradiant emission. The steady-state density matrix lives in a triangular state space characterized by quantum numbers J, M. Collective decay only leads to transitions in the same J manifold, whereas noncollective pumping and decay cause jumps to states in the same as well as adjacent J manifolds. (c),(d) Population distribution in J, M state space for $N=100$ atoms, for two states that are approximately equally subradiant [cf. Eq. (3)] but on either side of the phase transition.

space modes and the cavity mode as they decay to $|\downarrow\rangle$. Emission into free space is characterized by a jump operator $\sqrt{\gamma}\hat{\sigma}_j^-$ for each atom. Assuming that the atoms are identically coupled to the cavity mode, the emission of a cavity photon is characterized by the jump operator $\sqrt{\Gamma_c}\hat{J}^-$ where $\hat{J}^-=\sum_{j=1}^N\hat{\sigma}_j^-$ is the collective angular momentum lowering operator. Here, $\Gamma_c=C\gamma$ is the single atom emission rate into the cavity, which is modified by the dimensionless cooperativity parameter C. The decay channels are balanced by an effective incoherent pumping of the individual atoms from $|\downarrow\rangle\rightarrow|\uparrow\rangle$ which is represented by a jump operator $\sqrt{w}\hat{\sigma}_j^+$ for each atom. The master equation governing the spin dynamics is therefore given by

$$\partial_t\hat{\rho}=\sum_{j=1}^N\hat{\mathcal{D}}\left[\sqrt{w}\hat{\sigma}_j^+\right]\hat{\rho}+\sum_{j=1}^N\hat{\mathcal{D}}\left[\sqrt{\gamma}\hat{\sigma}_j^-\right]\hat{\rho}+\hat{\mathcal{D}}[\sqrt{\Gamma_c}\hat{J}^-]\hat{\rho}, \tag{1}$$

where $\hat{\mathcal{D}}[\hat{O}]\hat{\rho}=\hat{O}\,\hat{\rho}\,\hat{O}^\dagger-\hat{O}^\dagger\hat{O}\,\hat{\rho}\,/2-\hat{\rho}\hat{O}^\dagger\hat{O}/2$ is the Lindblad dissipator associated with a jump operator $\hat{O}$.

This master equation is invariant under permutations of the atomic indices and this symmetry results in a drastic reduction of the Liouville space for the steady-state solution from 4^N to $\mathcal{O}(N^3)$ basis states [30,31]. Furthermore, the master equation also possesses a $U(1)$ symmetry which can be seen by making the transformation $\hat{\sigma}_j^\pm\rightarrow e^{\pm i\phi}\hat{\sigma}_j^\pm$ in Eq. (1). This additional symmetry reduces the required basis states to $\mathcal{O}(N^2)$.

A convenient representation of these basis states uses the permutation invariant eigenstates of the $\hat{\mathbf{J}}^2$ and $\hat{J}^z$ operators with respective quantum numbers J, M [32]. Here, we have introduced the collective angular momentum components $\hat{J}^i=\sum_{j=1}^N\hat{\sigma}_j^i/2$, $i=x,\ y,\ z$, wherein $\hat{\sigma}_j^x=\hat{\sigma}_j^++\hat{\sigma}_j^-$ and $\hat{\sigma}_j^y=-i(\hat{\sigma}_j^+-\hat{\sigma}_j^-)$. The two quantum numbers $J=0,1,2,\ldots,N/2$ (for an even N [35]) and $M=-J,\ldots,J$ form a discrete, triangular state space for the collective atomic state in Liouville space as shown in Fig. 1(b). While the two vertices at $J=N/2$, $M=\pm N/2$ correspond to trivial product states with all spins in $|\uparrow\rangle$ or $|\downarrow\rangle$, the third vertex at $J=0$, $M=0$ is a highly entangled, subradiant state wherein the atoms are grouped into $N/2$ singlet pairs [36].

In this state space, collective emission leads to a transition with $\Delta M=-1$ within a ladder of constant J. While the free space emission and repump of any single atom breaks permutation invariance, the cumulative effect of either of these processes occurring for all atoms preserves this symmetry. Hence, they can be viewed as transitions between different states in this state space with $\Delta M=-1,\ +1$ respectively. Crucially, these processes couple adjacent J ladders and take the system away from $J=N/2$ which is the initial value when the atomic pseudospins are initialized in a coherent spin state. Closed form expressions for the transition probabilities [37] enable us to numerically determine the steady-state by exact diagonalization (ED) of a rate matrix [32].

Signatures of the phase transition.—For repump rates such that $\gamma+\Gamma_c<w<N\Gamma_c$, the system is in the superradiant regime that is characterized by positive inversion and spin-spin correlations $\langle\hat{\sigma}_1^z\rangle$, $\langle\hat{\sigma}_1^+\hat{\sigma}_2^-\rangle>0$ [1]. We now vary w in the weak repump regime $0<w<\gamma+\Gamma_c$ while keeping the values of γ, Γ_c fixed. We choose $\gamma/\Gamma_c=0.1$, corresponding to $C=10$. We first consider the cavity output power per atom, which is proportional to $\langle\hat{J}^+\hat{J}^-\rangle/N$, where $\hat{J}^+=(\hat{J}^-)^\dagger$. Figure 2(a) plots this quantity for different atom numbers as w is scanned across γ. With increasing system size, we observe signatures of a nonanalytic change at $w=\gamma$ that indicates a phase transition. We use second-order cumulant theory to obtain analytical insight into this behavior. Using an expansion in the small parameter $1/N$, we find that the $\mathcal{O}(N^0)$ behavior of $\langle\hat{J}^+\hat{J}^-\rangle$ is given by [32]

$$\langle\hat{J}^+\hat{J}^-\rangle=\begin{cases}0 & 0<w<\gamma\\ N\frac{w-\gamma}{2\Gamma_c} & \gamma<w<\gamma+\Gamma_c.\end{cases} \tag{2}$$

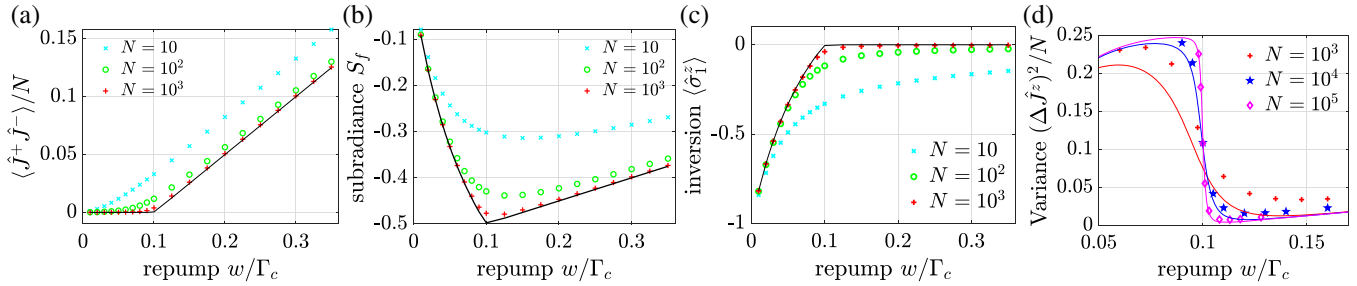

FIG. 2. Signatures of the phase transition. (a) Cavity power output per atom, characterized by $\langle \hat{J}^+\hat{J}^-\rangle/N$, (b) Subradiance factor S_f and (c) Mean atomic inversion, as w is scanned across $\gamma(=0.1\Gamma_c)$. Markers show the results from exact diagonalization for various atom numbers. The solid line is the result for $N = 10^5$ atoms obtained using second-order cumulant theory. (d) Normalized variance of the total inversion. The solid lines in (d) are computed using third-order cumulant theory for the displayed atom numbers.

For $w < \gamma$, a zero solution at leading order reveals the strong suppression of the cavity output power, which does not grow with N in this regime. On the other hand, the output power grows linearly with N for $w > \gamma$.

Importantly, the critical point $w = \gamma$ is distinct from and precedes the onset of superradiance at $w = \gamma + \Gamma_c$. As a result, the collective atomic state is subradiant (with respect to emission into the cavity) in both the phases demarcated by this point. A quantitative measure of the degree of subradiance is the per-atom reduction in the collective emission rate in units of Γ_c. This subradiance factor S_f is given by

$$S_f = \frac{1}{N}\left[\langle \hat{J}^+\hat{J}^-\rangle - \left(\frac{N}{2} + \langle \hat{J}^z\rangle\right)\right] = (N-1)\langle\hat{\sigma}_1^+\hat{\sigma}_2^-\rangle, \quad (3)$$

where $\langle \hat{J}^+\hat{J}^-\rangle$ describes collective emission and includes the effects of atom-atom correlations, while the second term describes the emission from N uncorrelated atoms. The $J = 0, M = 0$ singlet state gives the minimum possible value of $S_f = -0.5$ and hence it can be considered the most subradiant state. Remarkably, as shown in Fig. 2(b), we find that near the critical point $S_f \to -0.5$ with increasing system size, indicating that the system is highly subradiant on either side of this point and occupies states with J close to zero.

To understand how these two subradiant phases differ, we plot the population in the J, M states for $N = 100$ atoms at two points with similar values of $S_f(\approx -0.37)$ on either side of the critical point [Figs. 1(c) and 1(d)]. For $w < \gamma$, the population is localized around a mean $J \sim \mathcal{O}(N)$ and therefore even single collective excitations rapidly decay at a collectively enhanced decay rate $\sim J\Gamma_c$, largely confining the population to dark states with $M = -J$ [38]. In contrast, for $w > \gamma$, the collective decay is unable to confine the population to the lower boundary. In this regime, the system occupies states with vanishing values of J/N whereas all allowed M values are significantly populated, hence allowing the atoms to emit light through the cavity. To summarize, as w increases, the subradiant system "walks" up the lower boundary of the triangular state space, encounters the vertex at $J = 0$, and undergoes a phase transition into a qualitatively different family of subradiant states. Therefore, the phase transition arises as a result of the closed bottleneck at $J = 0$ that reflects the incoming population back into the $J \geq 0$ space (see animation [32]).

A nonanalytic change is also observed in the mean atomic inversion $\langle\hat{\sigma}_1^z\rangle = 2\langle\hat{J}^z\rangle/N$, plotted in Fig. 2(c). We find that $\langle\hat{\sigma}_1^z\rangle$ monotonically increases with w for $w < \gamma$ while it is essentially zero (at leading order) for $w > \gamma$ [32]. Further, a dramatic evidence for the phase transition is observed in the normalized variance of the collective inversion, given by $(\Delta\hat{J}^z)^2/N$. Figure 2(d) plots this quantity for $N = 10^3$, 10^4, 10^5 spins. Since $J \ll N/2$ in the critical region, we are able to extend the ED computation to $N \sim 10^5$ by working in a truncated state space with $J_{\max} \leq 1250$. With increasing atom number, we find strong evidence for a discontinuous jump in this quantity at the critical point. In cumulant theory, we find that this jump in the variance is only reproduced by accounting for third-order cumulants [32]. In particular, we cannot factorize three-atom correlations as $\langle\hat{\sigma}_1^+\hat{\sigma}_2^-\hat{\sigma}_3^z\rangle \approx \langle\hat{\sigma}_1^+\hat{\sigma}_2^-\rangle\langle\hat{\sigma}_1^z\rangle$. The nonanalytic behavior of the inversion and the discontinuity in the variance at the critical point are reminiscent of the behavior of order parameters and susceptibilities in equilibrium phase transitions, but in this system these features manifest in a strongly out-of-equilibrium setting.

Entanglement.—The failure of simple mean-field theory to reveal subradiance motivates us to investigate the entanglement properties of the steady state in this regime and in particular near the critical point $w = \gamma$. Since the system occupies states with $J \ll N/2$ near this point, an appropriate entanglement witness is the generalized spin squeezing parameter [40,41] given by

$$\xi^2 = \frac{(\Delta\hat{J}^x)^2 + (\Delta\hat{J}^y)^2 + (\Delta\hat{J}^z)^2}{N/2}, \quad (4)$$

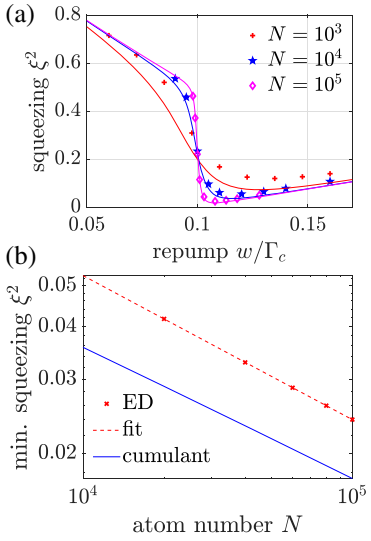

FIG. 3. (a) Steady-state squeezing parameter ξ^2 as w is scanned across $\gamma(=0.1\Gamma_c)$. Markers depict ED results while the lines are obtained from third-order cumulant theory. (b) Minimum ξ^2 value extracted from ED and third-order cumulant theory. A fit to the ED data reveals a scaling of $N^{-0.34}$.

where $(\Delta\hat{J}^i)^2 = \langle(\hat{J}^i)^2\rangle - \langle\hat{J}^i\rangle^2$ is the variance in the spin component $i = x, y, z$. A value of $\xi^2 < 1$ is sufficient to establish entanglement. Physically, this parameter captures the simultaneous compression of uncertainties in the three angular momentum components and takes the minimum value of $\xi^2 = 0$ for the macroscopic singlet state with $J = 0$, $M = 0$. Furthermore, ξ^2 also serves as an upper bound for the fraction of unentangled spins in the system [42].

Figure 3(a) plots ξ^2 as w is varied across γ. The discontinuity in $(\Delta\hat{J}^z)^2$ also manifests here as a sudden drop in ξ^2 near the critical point that becomes more pronounced with increasing system size. For a finite N, the minimum attainable ξ^2 decreases with N. As shown in Fig. 3(b), we find a power law scaling $\xi^2 \propto N^{-0.34}$ for the minimum value obtained using ED, which is approximately reproduced by the numerical solution of third-order cumulant theory where $\xi^2 \propto N^{-0.31}$. This scaling indicates that the fraction of unentangled spins, for which ξ^2 is an upper bound, vanishes as $N \to \infty$. Indeed, in the large N limit, we analytically find that $\xi^2 \to 0$ ($\xi^2 \to 1/2$) as $w \to \gamma^+$ ($w \to \gamma^-$) [32]. The subradiant-to-subradiant phase transition is thus characterized by macroscopic entanglement in the atomic ensemble where $O(N)$ atoms are entangled with other atoms.

Practical considerations.—Bad cavity lasers based on Raman transitions [3] as well as narrow-line optical transitions [43] can be potentially adapted to observe this transition. Experiments could also be based on cooperative emission from artificial atoms such as nitrogen-vacancy centers or quantum dots [44,45]. Whereas for steady-state superradiance the bad cavity requirement is $\kappa \gg N\Gamma_c$, with κ the cavity linewidth and $N\Gamma_c$ the order of the collectively enhanced single-atom emission rate, future studies can explore if this requirement can be relaxed in the subradiant regime where there is no such enhancement. However, similar to the superradiant regime, steady-state subradiance requires the atom-cavity system to satisfy $NC \gg 1$ but operate in the less explored weak pumping limit given by $w \sim \gamma \ll N\Gamma_c$. Although we have considered the stricter (but achievable [46]) condition $C > 1$ in this work, the nonanalytic behavior of the inversion and output power is independent of C, and the critical scaling of the minimum squeezing with N will also be observable for $C \lesssim 1$, albeit with an exponent of smaller magnitude [32]. However, for $C \ll 1$, the interval $\gamma < w < \gamma + \Gamma_c$ is very small and hence the subradiant-to-subradiant transition is immediately succeeded by the onset of superradiance. We have verified that the mean inversion, output power, and the minimum squeezing are robust to T_2 dephasing even when $1/T_2 \gtrsim \gamma$ [32]. The steady state is also robust to small fluctuations in the atom-cavity detuning since the resulting spin exchange Hamiltonian ($\propto \hat{J}^+\hat{J}^-$) is permutation and $U(1)$ symmetric and hence commutes with the steady-state density matrix. While $\langle\hat{J}^+\hat{J}^-\rangle$ can be inferred from the cavity output power, the mean inversion and the variance $(\Delta\hat{J}^z)^2$ could be measured, for instance, by preparing the steady state and subsequently measuring the population statistics in one of the pseudospin states by detecting the fluorescence from a cycling transition. Alternatively, quantum nondemolition (QND) schemes could also be used to measure the latter two observables [47,48]. The quantities S_f and ξ^2 can be estimated by combining these three quantities. The cavity output can also be used to measure photon bunching via the second-order correlation function $g^{(2)}(0)$, which we find exhibits an abrupt spike at the critical point [32].

So far, we have considered the case when atoms are identically coupled to the cavity mode, which can be achieved, e.g., by using a commensurate trapping wavelength [47] or by spectroscopic selection of atoms with near-maximal coupling [49]. We now briefly comment on the case of inhomogeneous atom-cavity coupling. Remarkably, we find that the cavity output power and the mean inversion in both phases remain unchanged at leading order even when the atoms are assumed to be arbitrarily distributed over a cavity mode wavelength [32]. The two phases still remain subradiant, although the expression for S_f must now account for the inhomogeneity. It may nevertheless be estimated using the output power and the mean atomic inversion [32]. Verifying entanglement may be possible by using a modified squeezing parameter that accounts for the spatial modulation entering the accessible observables as a result of the inhomogeneous coupling. We construct a modified squeezing parameter in the Supplemental Material [32], using which one could explore the possibility to detect entanglement in an inhomogeneously coupled system in future work.

Conclusion and outlook.—We have demonstrated that a bad cavity laser undergoes a dissipative phase transition from one subradiant phase to another before the onset of superradiance. Rather than destroying atomic correlations, single atom pumping and decay instead play a central role in generating and maintaining the entangled subradiant states we observe, which, in addition, are also robust to T_2 dephasing. Buoyed by recent experiments [50], subradiance is an exciting frontier with a variety of proposed applications such as ultrafast readouts [51], engineering of optical metamaterials [52], photon storage [53,54], quantum state transfer [55], and improved quantum metrology [56], to name but a few. In light of its robust nature, it will be interesting to explore potential applications of steady-state subradiance in quantum information processing, especially considering the features near the critical point such as a vanishing fraction of unentangled spins and an extreme sensitivity of observables to system parameters. From a fundamental perspective, it will be interesting to explore connections with quantum simulations of magnetism [57], topological properties of classical Markov chains [58,59], and higher-spin models, where a higher-dimensional state space potentially allows for even richer physics.

We thank Peter Zoller, Walter Hahn, John Cooper, James Thompson, and Ana Maria Rey for helpful discussions. A. S. acknowledges support from the European Union's Horizon 2020 research and innovation programme under Grant Agreement No. 731473 (FWF QuantERA via QTFLAG I03769). We also acknowledge support from the NSF AMO Grant No. 1806827; NSF PFC Grant No. 1734006; and the DARPA and ARO Grant No. W911NF-16-1-0576.

A. S. and J. T. R. contributed equally to this work.

*Corresponding author.
athreya.shankar@uibk.ac.at

[1] D. Meiser, J. Ye, D. R. Carlson, and M. J. Holland, Prospects for a Millihertz-Linewidth Laser, Phys. Rev. Lett. **102**, 163601 (2009).

[2] D. Meiser and M. J. Holland, Steady-state superradiance with alkaline-earth-metal atoms, Phys. Rev. A **81**, 033847 (2010).

[3] J. G. Bohnet, Z. Chen, J. M. Weiner, D. Meiser, M. J. Holland, and J. K. Thompson, A steady-state superradiant laser with less than one intracavity photon, Nature (London) **484**, 78 (2012).

[4] H. Liu, S. B. Jäger, X. Yu, S. Touzard, A. Shankar, M. J. Holland, and T. L. Nicholson, Rugged mHz-Linewidth Superradiant Laser Driven by a Hot Atomic Beam, Phys. Rev. Lett. **125**, 253602 (2020).

[5] J. A. Acebrón, L. L. Bonilla, C. J. Pérez Vicente, Félix Ritort, and R. Spigler, The Kuramoto model: A simple paradigm for synchronization phenomena, Rev. Mod. Phys. **77**, 137 (2005).

[6] C. von Cube, S. Slama, D. Kruse, C. Zimmermann, Ph. W. Courteille, G. R. M. Robb, N. Piovella, and R. Bonifacio, Self-Synchronization and Dissipation-Induced Threshold in Collective Atomic Recoil Lasing, Phys. Rev. Lett. **93**, 083601 (2004).

[7] B. Zhu, J. Schachenmayer, M. Xu, F. Herrera, J. G. Restrepo, M. J. Holland, and A. M. Rey, Synchronization of interacting quantum dipoles, New J. Phys. **17**, 083063 (2015).

[8] G. Heinrich, M. Ludwig, J. Qian, Björn Kubala, and F. Marquardt, Collective Dynamics in Optomechanical Arrays, Phys. Rev. Lett. **107**, 043603 (2011).

[9] M. Xu, D. A. Tieri, E. C. Fine, J. K. Thompson, and M. J. Holland, Synchronization of Two Ensembles of Atoms, Phys. Rev. Lett. **113**, 154101 (2014).

[10] M. Xu and M. J. Holland, Conditional Ramsey Spectroscopy with Synchronized Atoms, Phys. Rev. Lett. **114**, 103601 (2015).

[11] J. M. Weiner, K. C. Cox, J. G. Bohnet, and J. K. Thompson, Phase synchronization inside a superradiant laser, Phys. Rev. A **95**, 033808 (2017).

[12] B. Bellomo, G. L. Giorgi, G. M. Palma, and R. Zambrini, Quantum synchronization as a local signature of super- and subradiance, Phys. Rev. A **95**, 043807 (2017).

[13] A. Patra, B. L. Altshuler, and E. A. Yuzbashyan, Driven-dissipative dynamics of atomic ensembles in a resonant cavity: Nonequilibrium phase diagram and periodically modulated superradiance, Phys. Rev. A **99**, 033802 (2019).

[14] A. Patra, B. L. Altshuler, and E. A. Yuzbashyan, Chaotic synchronization between atomic clocks, Phys. Rev. A **100**, 023418 (2019).

[15] K. Tucker, B. Zhu, R. J. Lewis-Swan, J. Marino, F. Jimenez, J. G. Restrepo, and A. M. Rey, Shattered time: can a dissipative time crystal survive many-body correlations?, New J. Phys. **20**, 123003 (2018).

[16] P. Domokos and H. Ritsch, Collective Cooling and Self-Organization of Atoms in a Cavity, Phys. Rev. Lett. **89**, 253003 (2002).

[17] A. T. Black, H. W. Chan, and V. Vuletić, Observation of Collective Friction Forces Due to Spatial Self-Organization of Atoms: From Rayleigh to Bragg Scattering, Phys. Rev. Lett. **91**, 203001 (2003).

[18] H. W. Chan, A. T. Black, and V. Vuletić, Observation of Collective-Emission-Induced Cooling of Atoms in an Optical Cavity, Phys. Rev. Lett. **90**, 063003 (2003).

[19] M. Xu, S. B. Jäger, S. Schütz, J. Cooper, G. Morigi, and M. J. Holland, Supercooling of Atoms in an Optical Resonator, Phys. Rev. Lett. **116**, 153002 (2016).

[20] S. B. Jäger, M. Xu, S. Schütz, M. J. Holland, and G. Morigi, Semiclassical theory of synchronization-assisted cooling, Phys. Rev. A **95**, 063852 (2017).

[21] C. Hotter, D. Plankensteiner, L. Ostermann, and H. Ritsch, Superradiant cooling, trapping, and lasing of dipole-interacting clock atoms, Opt. Express **27**, 31193 (2019).

[22] H. Ritsch, P. Domokos, F. Brennecke, and T. Esslinger, Cold atoms in cavity-generated dynamical optical potentials, Rev. Mod. Phys. **85**, 553 (2013).

[23] K. Baumann, C. Guerlin, F. Brennecke, and T. Esslinger, Dicke quantum phase transition with a superfluid gas in an optical cavity, Nature (London) **464**, 1301 (2010).

[24] K. J. Arnold, M. P. Baden, and M. D. Barrett, Self-Organization Threshold Scaling for Thermal Atoms Coupled to a Cavity, Phys. Rev. Lett. **109**, 153002 (2012).
[25] S. B. Jäger, J. Cooper, M. J. Holland, and G. Morigi, Dynamical Phase Transitions to Optomechanical Superradiance, Phys. Rev. Lett. **123**, 053601 (2019).
[26] S. B. Jäger, M. J. Holland, and G. Morigi, Superradiant optomechanical phases of cold atomic gases in optical resonators, Phys. Rev. A **101**, 023616 (2020).
[27] D. Meiser and M. J. Holland, Intensity fluctuations in steady-state superradiance, Phys. Rev. A **81**, 063827 (2010).
[28] V. V. Temnov and U. Woggon, Photon statistics in the cooperative spontaneous emission, Opt. Express **17**, 5774 (2009).
[29] A. Auffèves, D. Gerace, S. Portolan, A. Drezet, and M. F. Santos, Few emitters in a cavity: from cooperative emission to individualization, New J. Phys. **13**, 093020 (2011).
[30] M. Xu, D. A. Tieri, and M. J. Holland, Simulating open quantum systems by applying SU(4) to quantum master equations, Phys. Rev. A **87**, 062101 (2013).
[31] N. Shammah, S. Ahmed, N. Lambert, S. De Liberato, and F. Nori, Open quantum systems with local and collective incoherent processes: Efficient numerical simulations using permutational invariance, Phys. Rev. A **98**, 063815 (2018).
[32] See Supplemental Material at http://link.aps.org/supplemental/10.1103/PhysRevLett.127.073603, which includes Refs. [33,34], for more details, and for an animation of the changing population distribution in the J, M states as w is scanned across γ.
[33] L. Mandel and E. Wolf, *Optical Coherence and Quantum Optics* (Cambridge University Press, Cambridge, England, 1995), https://doi.org/10.1017/CBO9781139644105.
[34] J. Cooper and A. Szöke, Effect of laser bandwidth on intense-field raman scattering, Phys. Rev. A **23**, 378 (1981).
[35] This assumption is purely for computational convenience and for simplifying the presentation. Our results are valid for any N in the $N \gg 1$ regime which is considered here.
[36] I. Urizar-Lanz, P. Hyllus, I. L. Egusquiza, M. W. Mitchell, and G. Tóth, Macroscopic singlet states for gradient magnetometry, Phys. Rev. A **88**, 013626 (2013).
[37] Y. Zhang, Y.-X. Zhang, and K. Mølmer, Monte-carlo simulations of superradiant lasing, New J. Phys. **20**, 112001 (2018).
[38] A similar population distribution has been previously reported in an atom-cavity system with coherent atomic driving [39].
[39] M. Gegg, A. Carmele, A. Knorr, and M. Richter, Superradiant to subradiant phase transition in the open system dicke model: Dark state cascades, New J. Phys. **20**, 013006 (2018).
[40] G. Tóth, C. Knapp, O. Gühne, and H. J. Briegel, Optimal Spin Squeezing Inequalities Detect Bound Entanglement in Spin Models, Phys. Rev. Lett. **99**, 250405 (2007).
[41] G. Tóth, C. Knapp, O. Gühne, and H. J. Briegel, Spin squeezing and entanglement, Phys. Rev. A **79**, 042334 (2009).
[42] G. Tóth and M. W. Mitchell, Generation of macroscopic singlet states in atomic ensembles, New J. Phys. **12**, 053007 (2010).
[43] M. A. Norcia and J. K. Thompson, Cold-Strontium Laser in the Superradiant Crossover Regime, Phys. Rev. X **6**, 011025 (2016).
[44] A. Angerer, K. Streltsov, T. Astner, S. Putz, H. Sumiya, S. Onoda, J. Isoya, W. J. Munro, K. Nemoto, Jörg Schmiedmayer, and J. Majer, Superradiant emission from colour centres in diamond, Nat. Phys. **14**, 1168 (2018).
[45] M. Scheibner, T. Schmidt, L. Worschech, A. Forchel, G. Bacher, T. Passow, and D. Hommel, Superradiance of quantum dots, Nat. Phys. **3**, 106 (2007).
[46] A. Kawasaki, B. Braverman, E. Pedrozo-Peñafiel, C. Shu, S. Colombo, Z. Li, Ö. Özel, W. Chen, L. Salvi, A. Heinz, D. Levonian, D. Akamatsu, Y. Xiao, and V. Vuletić, Geometrically asymmetric optical cavity for strong atom-photon coupling, Phys. Rev. A **99**, 013437 (2019).
[47] O. Hosten, N. J. Engelsen, R. Krishnakumar, and M. A. Kasevich, Measurement noise 100 times lower than the quantum-projection limit using entangled atoms, Nature (London) **529**, 505 (2016).
[48] K. C. Cox, G. P. Greve, J. M. Weiner, and J. K. Thompson, Deterministic Squeezed States with Collective Measurements and Feedback, Phys. Rev. Lett. **116**, 093602 (2016).
[49] B. Wu, G. P. Greve, C. Luo, and J. K. Thompson, Site-dependent selection of atoms for homogeneous atom-cavity coupling, arXiv:2104.01201.
[50] W. Guerin, M. O. Araújo, and R. Kaiser, Subradiance in a Large Cloud of Cold Atoms, Phys. Rev. Lett. **116**, 083601 (2016).
[51] M. O. Scully, Single Photon Subradiance: Quantum Control of Spontaneous Emission and Ultrafast Readout, Phys. Rev. Lett. **115**, 243602 (2015).
[52] J. Rui, D. Wei, A. Rubio-Abadal, S. Hollerith, J. Zeiher, D. M. Stamper-Kurn, C. Gross, and I. Bloch, A subradiant optical mirror formed by a single structured atomic layer, Nature (London) **583**, 369 (2020).
[53] G. Facchinetti, S. D. Jenkins, and J. Ruostekoski, Storing Light with Subradiant Correlations in Arrays of Atoms, Phys. Rev. Lett. **117**, 243601 (2016).
[54] A. Asenjo-Garcia, M. Moreno-Cardoner, A. Albrecht, H. J. Kimble, and D. E. Chang, Exponential Improvement in Photon Storage Fidelities using Subradiance and "Selective Radiance" in Atomic Arrays, Phys. Rev. X **7**, 031024 (2017).
[55] P.-O. Guimond, A. Grankin, D. V. Vasilyev, B. Vermersch, and P. Zoller, Subradiant Bell States in Distant Atomic Arrays, Phys. Rev. Lett. **122**, 093601 (2019).
[56] L. Ostermann, H. Ritsch, and C. Genes, Protected State Enhanced Quantum Metrology with Interacting Two-Level Ensembles, Phys. Rev. Lett. **111**, 123601 (2013).
[57] A. Chiocchetta, D. Kiese, F. Piazza, and S. Diehl, Cavity-induced quantum spin liquids, arXiv:2009.11856.
[58] K. Dasbiswas, K. K. Mandadapu, and S. Vaikuntanathan, Topological localization in out-of-equilibrium dissipative systems, Proc. Natl. Acad. Sci. U.S.A. **115**, E9031 (2018).
[59] A. Murugan and S. Vaikuntanathan, Topologically protected modes in non-equilibrium stochastic systems, Nat. Commun. **8**, 13881 (2017).